

Experimental Study of Air-Lift Pumps Characteristics

Naji F. Al-Sager & Mohammed E. Al-Shibani

Public Authority of Applied Education and Training

Abstract

The main aim of this work is to study the Air-lift pumps characteristics according to design parameters such as the percentage of the distance between throat section and nozzle and the driving air pressure, suction head and also study the effect of each parameter on the air lift pump characteristics in order to have a better performance of such pump under various conditions.

A certain geometry for air-lift pump designed and manufactured. The experiments show that there must be careful in increasing the suction head, and a balance must be considered between the suction head and the driving air volumetric flow rate. While the effect of increasing air pressure will stop at certain maximum of the ratio of the volumetric flow rate of water and air that is any increase in air pressure will meet no change ratio of the volumetric flow rate of water and air, While Increasing S/Dth will leads to decrease in the percentage of ratio of the volumetric flow rate of water and air because the optimum S/Dth so that at this value we will have the best performance and any other values for S/Dth the percentage of ratio of the volumetric flow rate of water and air will decreases , but this effect is not so clear and it could be neglected. The pump performance is not so sensitive with the change of S/Dth after a certain value, this information will help in the use of the air-lift pump in several applications using the predetermined operating conditions.

I. INTRODUCTION

Air-lift pump is a high volume flow rate pump. Simplicity of design, absence of any moving parts, ability to handle muddy water, reliability, ruggedness and low cost, more than compensate for the relatively poor efficiency of the pump, jet pump is the common part of the air-lift pump.

There has been little commercial interest in the development of low area jet pumps because of their characteristically low head rise. The basic components of the pump are inlet nozzle, throat and diffuser.

Beside that, the air lift pump or the pump applications through industry are numerous to mention but some of the most common ones are, in power stations it has been considered as an auxiliary boost pump in Rankin cycle, in ventilation and air conditioning, pneumatic or hydraulic conveyance of products in power form, coal and cinder transport in power plants, pumping of slug from shafts bore holes and pits, solid handling eductor is a special type called a hopper eductor, pumping sand from filter beds, sparkler nozzle is the simplest type of eductors and steam lined eductors used to remove condensate from vessels under vacuum.

Sadek Z. Kassaba, Hamdy A. Kandila, Hassan A. Wardaa and Wael H. Ahmedb, (2008) show that the pump capacity and efficiency are functions of the air mass flow rate, submergence ratio, and riser pipe length. The best efficiency range of the air-lift pumps operation was found to be in the slug and slug-churn flow regimes. S. Z. Kassab1, H.

A. Kandil2, H. A. Warda3, W. A. Ahmed4,(2001) show that the experimental results showed that the maximum water flow rate increases when the submergence ratio and/or the riser pipe length is increased. The best efficiency range of the air lift pump operation was found to be in the slug and slug-churn flow regimes.

When either the well or the power fluid contains gas, E. Lisowski and H. Momeni (2010) use liquid as motive and driven fluids, it might be found a nozzle, where a motive fluid flows into the pump, entrainment where motive and driven fluids are mixing and finally discharge where both fluids leaves the pump. The same equations driven for incompressible liquids are used with modifying the mass flow rate ratio and the friction loss coefficients, in order to obtain an acceptable conformity between the theory and observation, we have to increase the hydraulic loss coefficient – up to 30 times for the present case study which is closed-conduits this level of correction has been determined by means of the trial and error method, Jerzy (2007). the pump acts as a sort of venture tube, where the velocity of the induced flow can be increased to a value close to that of the driving flow. This is favorable for high exchange efficiency between the two flows. The energy in the mixture can exceed the kinetic energy of the driving flow, which would expand freely to the total pressure of the induced flow, in such a way that the losses considerably influence the efficiency of the unit. Thus it is important to minimize losses by friction in the mixing section and converging losses

in the diffuser, both of which are proportional to the square of the velocity.

Static pressure (driving air pressure) at the entrance of the nozzle is converted to kinetic energy by permitting the fluid to flow freely through a converging nozzle. The resulting- high velocity stream entrains the suction fluid in the suction chamber where the driving air jet creates a vacuum in the plenum chamber upstream of the diffuser section, increasing of the velocity decreases the pressure value for the same stream line according to Bernoulli equation. Water is, thereby drawn from the suction tank through a flexible hose, resulting in a flow of mixed fluids (air and water) at an intermediate velocity. The diffuser section (at the top of the jet pump) converts the velocity back to static pressure at the discharge of the jet pump.

Standard jet pump uses an axial nozzle, a generally cylindrical mixture and a divergent diffuser with a small angle (7 to 8 degree). This is the simplest design, but one having the largest dimensions and poorest performance. Thus, different techniques should be examined to improve the efficiency and compactness.

Following are the major techniques listed in order to increase performance of the jet pump:

1. The pumps with partial injection of the driving fluid by an annular slot at the inlet of the mixture are well suited to the pneumatic conveyance of products or the extraction and cooling of the gasses.
2. Multi tube and BI-dimensional pump which can comprise three, seven, nine, 19, 37 and so for driving nozzles.
3. Annular jet pumps with thin divergent flow whose performance is comparable to that of jet pumps with seven or nine divergent injectors.
4. Jet pumps with several annular flows, concentric and divergent, whose compactness and performance with a diffuser are the best for jet pumps handling Uni. -Interrupted flows.
5. Pulse jet pump, which's driving flow, comprises successive-bursts or -blasts- of gasses sucking in waves of induced air, the efficiency can be high.

Most of the papers in the literature on the design of liquid-liquid jet pumps contain empirical information on the coefficient S/Dth .

1I. A. El-Sawaf, 2M. A. Halawa, 3M. A. Younes and 4I. R. Teaima (2011) Study the effects of the pump operating conditions and geometries on the performance, the experimental investigations that the pump head and the head ratio decrease with increasing suction capacity and the area ratio R (A_n/AMC) of 0.25 gives the maximum highest efficiency and the area ratio of 0.155 gives a lowest

efficiency. The optimum value for S/Dth for pumping water is about 1.

Ibrahim (2012) insure the same investigations and the driving pressure of 1 bar gives the maximum delivered concentration in case of $R=0.25$ and 0.4 but at $R= 0.155$ the driving pressure of 1.5 bar gives the maximum delivered concentration.

1-1-Consequences of Nozzle-Throat Interface

In addition to promoting cavitation, interference between the nozzle exterior and the throat entry interior surfaces is an important cause of the large losses in the jet pumps.

Ibrahim (2012), the distance between the driving nozzle to the beginning of mixing chamber to driving nozzle diameter ratio of 1.5 gives the maximum for all tested cases.

Mueller (1964) is one of the few investigators who measured the throat entry loss coefficient and his results graphically illustrate the profound effect of an adequate nozzle to throat spacing on the loss coefficient Ken (If $S/Dth = 0.55$ where the measured Ken value was 0.061).

When the nozzle is inserted to $S/Dth = 0.023$, the measured Ken values increased by an order of magnitude to 0.745, actually this radical increase in the throat entry loss coefficient reflects a combination of the main flow losses and a secondary flow losses.

1-2- Optimum Mixing Throat Length

Ibrahim (2012), the mixing chamber length of 7.25 D_{mix} had proven superiority over the other two mixing chamber length of 6.75 and 7.86 D_{mix} . Mixing throat length ranging from 3.5 to approximately 10 times the throat diameters has been studied. Vogel (1965) measured the static pressure rise in a very long throat length up to 20 diameters in length, his results illuminated an often over looked point that is the dependence of optimum throat length on the flow ratio M , regardless, of the design area ratio of the pump. For an area ratio of $R = 0.219$ he found that the pressure rise in the mixing throat is at 5.3 diameters at low secondary flows approaching the cut-off point, and the required or optimum mixing length increased many times the diameters at high values of the flow ratio m , i. e., under low Pd conditions. Schulz and Fasol in 1958 using a larger area of area ratio $R = 0.219$ found that the pressure peaked at $L/Dth = 4.2$ for (M) goes to zero as contracted with a required mixing length of $L/Dth > 8.3$ at a maximum flow ratio.

1-3- Interrelationship Between S/ Dth and L/ Dth

The mixing length required to achieve maximum pressure rise in the throat is properly viewed as the total distance from the tip of the nozzle to completion of mixing. i.e. ($S/Dth + L/Dth$). Note

that the optimum S/D_{th} increased from zero for the longest throat to 2.3 throat diameters for the shortest length. Since the L/D_{th} values declined at a more rapid rate than growth in S/D_{th} , The totals declined somewhat. Note that the peak efficiency was obtained with the intermediate case, i.e., 1 diameter spacing and a 5.66 diameter mixing throat length show in table (1) for two short-throat pumps.

The same trend is evident; namely, a reduction in throat length requires a doubling in nozzle to throat spacing. Sanger study provides further information on one of the undesirable effects of excessive S/D_{th} values when used with a long (7.25)-mixing throat. The corresponding static pressure profiles with $S/D_{th} = 0$ or 0.96 showed continuous pressure rise through the throat and leveling off at the exit, indicating an optimum length. In contrast, a similar profile with $S/D_{th} = 2.68$ resulted in a throat pressure rise, which peaked at about 4.5 diameters and then declined due to frictional losses in the throat.

1-4- Effect of nozzle-throat spacing on performance and theory-experiment comparisons

Unfortunately, the liquid pump is increasingly prone to cavitation as the throat spacing (S/D_{th}) is reduced to zero. Static pressure measurements at the throat entry show that zero spacing causes large pressure drops at the throat entry and consequently promotes cavitation.

For $S/D_{th} = 0$ optimum nozzle setting for pump efficiency.

A. H. Hammoud and A. A. Abdel Naby (2006) for nozzle to throat spacing to nozzle diameter ratio (L/D), the optimum pump performance was obtained for drive pressure of 1.5 bar, while increasing the motive pump pressure the pump performance decreased. V. P. sharma¹, S. Kumaraswamy*¹ and A. Mani² (2011), Nozzle to mixing tube spacing play an important role in the performance of the jet pump.

1-5- Cavitation

One of the most important problems in the design of the pump systems is the prediction of cavitation. The pressure at the throat entrance is always less than the suction head H_s for suction flows greater than zero. If the driving air pressure is reduced below the vapor pressure P_v of the fluid being pumped, cavitation will result. Since P_v is the minimum pressure that can be obtained at the throat entrance, the suction flow at this point is the maximum that can be obtained with the particular value of the suction head. Attempts to lower the driving air pressure below P_v by increasing the nozzle flow rate will simply lead to greater vapor volumes at P_v in the suction fluid.

Cavitation may be induced in a pump as a result of increased velocity of the primary jet or decreased suction port pressure or decreased delivery pressure, ¹X. Long, ²H. Yao, ³J. Zhao (2009) study the effect of cavitation on the pump performance they concludes that flow patterns in the throat pipe of liquid pump under operating limit are observed, while the axial pressure distribution along the wall of the pump are also measured. Based on the analysis of the observation and calculations of the distribution of the mach No, it can be concluded that the critical liquid-vapor two phase flow will occur when a jet pump works under the operating limit. In this situation, the velocity of mixed flow reaches the corresponding sound velocity. That's the reason why the outlet flow rate remains unchanged with the decrease of outlet pressure under a certain driving pressure when operating limits occurs.

Mixing throat cavitation in a liquid jet pump results from high jet velocity, low suction pressure (NPSH) or low Net Positive Suction Head developing cavitation at the jet boundary has no effect on the pump efficiency, but under severe conditions it spreads to the walls. Cavitation can be avoided by reducing V_n and R or by raising suction port pressure.

II. EXPERIMENTAL SET-UP AND MEASUREMENT

A new experimental-set up is constructed to investigate the effect of the design parameters on the pump performance in order to have a better understanding about the behavior of such pump under various conditions.

2-1- The set-up assembly:

The set-up assembly shown in figure (1) consists of the main following components:

1. Main compressed air valve.
2. Secondary compressed air tank.
3. Manometer.
4. Orifice meter.
5. Air-lift pump.
6. Delivered water tank.
7. Feed water tank.

A 500 liter pressurized air tank (2) is used as a main air tank (outside the laboratory) connected to a 150-liter tank as a secondary tank beside the system to increase the stable periods of the pressure feeding. The secondary tank is connected to the orifice meter through a flexible tube connected to the control valve, the orifice meter is connected to the nozzle-tube by a galvanized 18 mm pipe and a pressure gauge is placed just before the nozzle-tube to measure the driving air pressure.

To enable the nozzle-tube moving up and down to change the percentage S/D_{th} the lower flange figure (4) is threaded in the center by 2 mm fine

threads 38 mm hole. A 75 mm inside diameter, 30 mm length brass pipe is fabricated to connect the pump body to the lower and upper flanges, 4-holes 8 mm diameter drilled to enable connecting the pump parts together. The upper flange figure (5) is same as the lower flange. A 58 mm-pipe, 30 mm long is fabricated to be connected to the discharge line.

The orifice meter figure (6) designed according to the BRITISH STANDARD (BS-1042 Part-1 1964). It is used to measure the driving air flow rate by producing a pressure difference across an orifice placed between two tubes (Orifice meter) with $D_{oi} = 19$ mm, $D_{oo} = 70$ mm, the hole angle is 45° . Taping done at 28mm distance before the orifice and 14 mm distance after the orifice (according to the British Standard) placed between two 50 mm long Perspex pipes. The pressure difference across the orifice was measured by using mercury manometer; the orifice meter is calibrated using hydraulic bench. The upper tank (6) is $0.50 \times 0.50 \times 0.60$ m galvanized steel equipped with 0.25×0.25 m Opening at the top and a side glass to indicate the water level in the tank. The tank level is fixed by upper stand $1 \times 1 \times 1.1$ m over the lower stand, and the lower tank (7) is $0.50 \times 0.50 \times 0.60$ m, equipped with a floating valve at the inlet to control the water level in the tank (beside the presence of the over flow hole to insure a fixed water level).

Feeding of water through a 12.5 mm line connected to the control valve to maintain the water level constant in the feeding tank so that the suction head can be constant during operation.

The stagnation pressure inside the pressurized air tank is measured by a pressure gauge fixed on top of the tank, while the static pressure in the jet-nozzle tube is measured by a pressure gauge fixed on top of the tank.

2-1-1- The Air-lift Pump:

It consists of a converging diverging tubefabricated from Perspex plastic for visual observations studies, see figure (3). This type of material has ultimate tensile strength [UTS] of 40 – 75 MPa, the tube consists mainly from cylindrical entrance, inlet nozzle followed by long throat section, then a convergent section followed by the exit cylinder.

A50 mm tubes are welded just before the inlet convergent section for the inlet of suction fluid. The nozzle tube is fabricated from brass to avoid corrosion. It consists of a tube with a 38 mm outside diameter, 305 mm long and it is threaded from outside to engage with the lower flange as male and female. A 35 mm long 12 mm outlet diameter 20 mm inlet diameter brass nozzle is welded to the tube to have the pressurized air as a jet as shown in figure (7).

2-2- Measurements

2-2-1 Pressure

Stagnation pressure inside the pressurized air tank and Static pressure in the jet-nozzle tube are measured by using a Bourdon tube gauge fixed on the top of the tank. Measuring upstream air pressure using Bourdon pressure gauge with measuring range of 0-10 bar with $\pm 2\%$ of F.S., while downstream air pressure measured using Digital compound gauge with measuring range of $\pm 0.1\%$ F.S.

2-2-2- Measuring the discharged water mass flow rate (\square_w):

It is measured by collecting discharged water in the upper tank and by using the glass level indicator and the dimensions of the tank we can evaluate the water volume over a period of time (t) measured using digital stop watch, the process is repeated using calibrated rotameter then the discharged water mass flow rate can be evaluated .

2-2-3- Measuring the pressurized air mass flow rate (\square_a):

By measuring the pressure difference across the orifice in an calibrated orifice meter which inserted in the pressurized air feed line, the net vertical high difference can be measured using mercury filled U-tube manometer with measuring range 0-500 mm and ± 2 mm accuracy, then, the mass air flow rate can be evaluated. The orifice meter is calibrated using hydraulic bench to have a calibration curve for different values of the driving air mass flow rate.

III. RESULTS AND DISCUSSION

A series of tests done to calibrate the orifice meter by using hydraulic bench and collect water in a tank and calculate the time for this quantity of water to have the actual flow rate and compare it with the theoretical flow rate calculated theoretically. The mean value for the discharge coefficient C_d equal to 62.5, so that this value will be used as a constant value for the discharge coefficient in the driving air mass flow rate calculations.

The series of test in figure 8 (a, b, c, and d) shows the relation between \square_a , and \square_w at a constant $S/D_{th} = 0.5$ for different suction heads ($H_s = -10, 10, 20, 30$ Cm).

From the graph one can see that increasing \square_a shall increase \square_w at the same H_s , and as H_s increases the flow rate increases too. For the same \square_a , and the minimum water mass flow rate is at $H_s = -10$ Cm. For a certain value of H_s as \square_a increased, \square_w increased proportionally. If the throat pressure is constant at -10 Cm of water, increasing P_{US} shall

increase the flow rate up to the choking pressure, after which the flow rate shall remain constant. Same as the first series but at $S/D_{th} = 1.5$ and 3.0 respectively in figures (8, 9, 10) they show the same trend as described above.

Another Series in figure 9 (a, b, c, and d) show the variations of \square_w , against \square_a at $H_s = -10, 10, 20, 30$ Cm., at a constant $S/D_{th}=1.5$ The results (as shown in the figures) as expected, the tendency for the characteristics to reach a maximum followed by a slight fall before flattening off is clear particularly for the low pumping heads. The characteristic shape beyond an air mass flow rate of 1.1×10^{-2} Kg/sec (corresponding to a supply pressure of approximately 6.5 atm.) could not be established due to limitations. Another Series in figure 10 (a, b, c, and d) show the variations of \square_w , against \square_a at $H_s = -10, 10, 20, 30$ Cm., at a constant $S/D_{th}=3.0$ The results (as shown in the figures) as expected. For certain value of S/D_{th} as P_a increased, the dimensionless percentage M increased up to the maximum value, and then the curve falls down slowly. The graphs show that the maximum M at different values of S/D_{th} . Table (1) show the locations of maximum M at various driving pressure and suction head. In each series the three curves have the same trend.

IV. CONCLUSIONS

From all the previous results, different points can be calculated:

4-1- Effect of Water Head (H_s)

For this series of tests, the following values of the dimensionless geometric parameters are chosen:

$$S/d_1 = 0.5$$

$$L/d_2 = 5.12$$

$$d_2/d_1 = 2.25$$

It is clearly that for the same configuration of the system, increasing H_s lead to increase in \square_w for the same \square_a in Figure 8 (a, b, c, and d) proportionally, but the optimum performance is at $S/D_{th} = 0.5, H_s = 30$ Cm.

This is agreeing with the previous investigations done. Increasing H_s from -10 Cm to 30 Cm leads to decrease in M because of the required increase \square_a so that it could be concluded that there must be careful in increasing the suction head, and a balance must be considered between the suction head and the driving air mass flow rate.

4-2- Effect Of The Driving Air Pressure P_a

For the same S/D_{th} , H_s increasing the driving air pressure P_a leads to proportional increase in M up to the optimum region, and then increasing P_a will leads to decreases in M . This means that the driving air pressure must be limited otherwise it cause a

reverse effect. At the same P_a increasing H_s results in decreasing of M , at the same driving pressure P_a increasing the percentage S/D_{th} results in decreasing of the percentage of M . The effect of increasing P_a will stop at certain maximum of M that is any increase in the driving air pressure P_a will meet no change in M .

4-3- Effect Of The Percentage S/D_{th}

Increasing S/D_{th} will leads to decrease in the percentage of M because the optimum $S/D_{th} = 0.5$ so that at this value we will have the best performance and any other values for S/D_{th} the percentage M will decreases, but this effect is not so clear and it could be neglected. The pump performance is not so sensitive with the change of S/D_{th} after $S/D_{th} = 0.5$. It is important to mention here that $S/D_{th} = 0$ is the reason for high cavitation losses.

4-4- Effect of Hysteresis

From figure 8&9 (a, b, c, and d) for the two runs as a result of the presence of the Hysteresis phenomena there was a difference between the two runs because of the friction, and thermal effects. It could be summarized that: -

1. S/D_{th} should be of the order of 0.5 to 1.5 throat diameters.
2. Performance is insensitive in this range and a value of 1 is commonly recommended.
3. It is unlikely that commercial jet pumps will be constructed with S/D_{th} values of zero because of the cavitation penalty.

REFERENCES

- [1] H. Yano, I. Funaki, T. Shinoki, A. Kieda and S. Simotori (1990) "Performance of a New Type of Water Jet Pump", Transactions of ASME Journal, Vol (2), pp. 98-112.
- [2] I.J. Karassic, J.P. Messina, P. Cooper, C.C. Healed (2008) Pump Handbook, Fourth edition, McGraw-Hill, NY.
- [3] Mueller N. H. G., (1964) "Water Jet Pump" J. Am. Soc. Civil Eng. 90-HY3, 83.
- [4] Iran, E and Rodrigo E. (2004) "Performance of low-Cost Ejectors", Journal of Irrigation and Drainage Engineering. ASCE trans., pp.122-128. H. Hammoud, (2006) "Effect of Design and Operational parameters on The pump Performance", Beirut Arab University, Mechanical Engineering Department, Proceedings of the 4th WSEAS International Conference on fluid mechanics and Aerodynamics, Elounda, Greece, August 21-23, pp. 245-252.
- [5] Jerzy M. Sawicki (2007), "Hydraulic Loss Coefficient in 1D flows", University of Technology, Faculty of Civil and

- Environmental Engineering, Archives of Hydro-Engineering and Environmental Mechanics., Vol. 54, No. 2, pp. 95-116
- [6] ¹E. Lisowski and ²H. Momeni (2010), "CFD Modeling of a jet Pump with Circumferential Nozzles for Large Flow Rates", ¹Institute of Applied Informatics, Cracow University of Technology, Poland, ²Institute of Machine and Marine Technology, Bergen University College, Norway. Archives of Foundry Engineering Volume 10, Special Issue 3/2010. pp.69-72.
- [7] Vogal, R., (1965), "Theoretische und Experimentelle Untersuchungen as Strohlopparaten, Maschinenbautechnik, Berlin, Germany, Vol. 5, P. 619.
- [8] ¹I. A. El-Sawaf, ²M. A. Halawa, ³M. A. Younes and ⁴I. R. Teaima (2011), "Study of the Different Parameters that Influence on the Performance of Water Jet Pump", ¹Professor, Mechanical Power Engineering Department, Faculty of Engineering, Port-Said University, Egypt, ²Assistant Professor, Mechanical Power Engineering Department, Faculty of Engineering, Al-Azhar University, Egypt, ³Professor, MERI, NWRC, Egypt, ⁴Assistant Researcher, MERI, NWRC, Egypt. Fifteenth International Water Technology Conference IWTC 15, Alexandria Egypt.
- [9] ¹X. Long, ²H. Yao, ³J. Zhao (2009) "Investigation on Mechanism of Critical Cavitating Flow in Liquid Jer Pump Under Operating Limits" ¹School of Power and Mechanical Engineering, Wuhan University, China. ²Nuclear Power Qinsham Joint Venture Company Limited, Haiyan, China.
- ³National Microgravity Laboratory, Institute of Mechanics, Chinese Academy of Science, Beijing, China. International Journal of Heat and Mass Transfere 52 2415-2420
- [10] Ibrahim R. Teaima (2012) "A Central-Type Jet Pump Model For Wheat Grains Removing From Water Channels" Mechanical & Electrical Research Institute, National Water Research Center, Delta, Barrage, Egypt, Sixteenth International Water Technology Conference, IWTC 16, Turkey.
- [11] P. sharma¹, S. Kumaraswamy^{*1} and A. Mani² (2011), ¹ Hydroturbomachines Laboratory, Department of mechanical Engineering Indian Institute of Technology Madras, Chennai, India, ²Refrigeration & Air-conditioning Laboratory, Department of mechanical Engineering Indian Institute of Technology Madras, Chennai, India.
- [12] Sadek Z. Kassaba, Hamdy A. Kandila, Hassan A. Wardaa and Wael H. Ahmedb, (2008) " Air-lift pumps characteristics under two-phase flow conditions" aMechanical Engineering Department, Faculty of Engineering, Alexandria University Alexandria, Egypt, bNuclear Safety Solution Ltd., AMEC, 700 University Avenue, Toronto, Ontario, Canada M5G 1X6
- [13] S. Z. Kassab¹, H. A. Kandil², H. A. Warda³, W. A. Ahmed⁴, (2001) " Performance of an Airlift Pump Operating in Two-Phase Flow" Mechanical engineering department, faculty of engineering, Alexandria University, Egypt, ICFDP7-2001004.

I. APPINDIX

Basic Laws Used in Calculations:

6-1-Determining Driving Air Volumetric Flow Rate (Q_{air})

$$m_a = Y * F * C * A * \sqrt{2 * \rho_{US} (P_{US} - P_{DS})} \quad (Kg / sec).$$

$$Y = 1 - (0.041 + 0.35) \left(\frac{d_o}{D}\right)^4 \frac{(P_{u.s} - P_{D.S})}{P_{u.S}} * \frac{1}{1.4}$$

$$F = \sqrt{\frac{1}{1 - \left(\frac{d_o}{D}\right)^4}}$$

$$A = \text{Orifice area} = (\pi / 4) * d_o^2 \quad (m^2)$$

$$\rho_{u.s} = \frac{P_{u.p} (bar) * 10^4}{R(29.3) * T_{u.s} (K)}$$

$$H_{air} = Y * \left(\frac{\gamma_u}{\gamma_a} - 1 \right)$$

$$\gamma_u = 13.6$$

$$\gamma_a = \frac{1}{800}$$

$$W_{air} * H_{air} = W_{air} * Y * \left(\frac{\gamma_u}{\gamma_a} - 1 \right)$$

Where :-

$$Y = \frac{\text{Right reading} - \text{left reading}}{100}$$

$$W_{air} = (1/800) * 9800 = 12.25 \quad N/m^3$$

$$P_{u.S} - P_{D.S} = W_{air} * Y * \left(\frac{\gamma_u}{\gamma_a} - 1 \right) \quad \frac{N}{m^2}$$

$$= \frac{N}{m^2} * 10^{-5} \quad bar$$

6-2-Determining Water Volumetric Flow Rate

$$\text{Volume of water in the upper tank} = 50 \times 50 \times Z \quad (Cm^3)$$

where :-

$$50 (Cm) \times 50 (Cm) = \text{Upper tank base area}$$

$$Q_w = \frac{\text{Volume of water} * 10^{-6}}{\text{time}} \left(\frac{m^3}{sec} \right)$$

6-3- Calculation of The pump Efficiency

The pump efficiency can be obtained from the following equation derived by- Mueller (1964). It is similar to the expression obtained by Vogal (1965) except that the friction loss in the driving line and the bend loss in the suction line are included in Mueller equation, and the mixing chamber loss has been treated differently. This equation can be used generally to determine the behavior of the pump of a certain construction.

$$\eta = \frac{v \left\{ 2R \left[\frac{1-v}{1-R} \right]^2 + (1+Z_6 - Z_5) \left[\frac{R+v}{1+R} \right]^2 - v^2 \left[\frac{1}{C_s^2} + Z_4 + Z_6 \right] \right\}}{R \left\{ Z_1 + \frac{1}{C_m^2} + Z_5' v^2 - 2R' \left[\frac{1-v}{1-R} \right]^2 - (1-Z_6 - Z_5' - Z_5'') \left[\frac{R'+v}{1+R'} \right]^2 \right\}}$$

Where:

For the specific geometry constructed in the present study $v = 1/2.25$

For $L_m = 14.35 \text{ Cm}$

1- Friction loss in driving line $Z_1 = 0.0012$

- 2- Driving nozzle loss $C_m = 0.94$
 $1/C_m^2 = 1.1316$
- 3- Suction nozzle loss $C_s = 0.757$
 $1/C_s^2 = 1.745$
- 4- Bend loss in suction line $Z_4 = 0.0026$
- 5- Friction loss in mixing chamber $Z'_5 = 0.0288$
 $Z''_4 = 0.0233$
- 6- Diffuser loss $Z_6 = 0.0835$

All the parameters values from Mueller tables for the efficiency equation.

Table (1)

| Reference | Throat entry shape | L / D _{th} |
|--------------------|--|---------------------|
| Vogal and Sanger | Conical, approx. 200° | 6 |
| Schultz and Fasol | Conical, 120° | 4 |
| Mueller | Rounded, radius = 0.9 / D _{th} | 6 – 7.5 |
| Vogal | Conical (180°), elliptical | 8.3 |
| Cunningham | 3 Conical (180°·90°·40°) One rounded radius = 2 D _{th} | 6 – 8 |
| Hansen and Kinnavy | Conical, 40° | 4.1 |
| Sanger | Rounded, radius = 3.7 D _{th} | 3.54 , 5.66 , 7.25 |

In all cases, corners are rounded at transitions (Cunningham and Sanger)

Figure (1) Schematic diagram of the set-up assembly

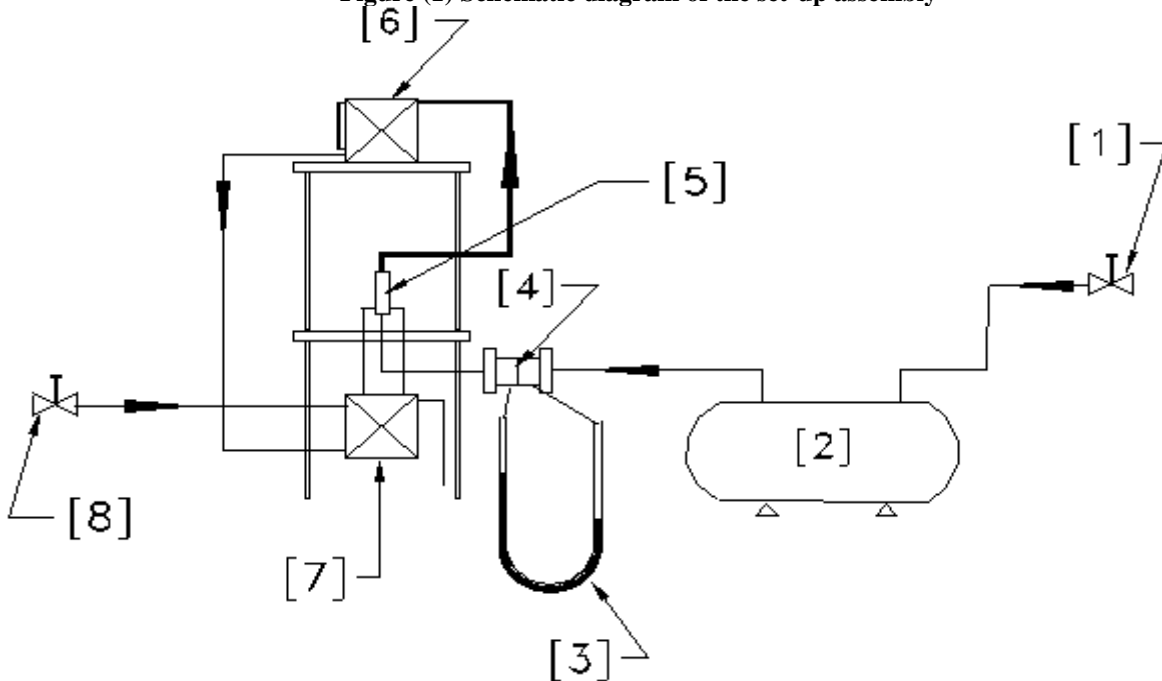


Figure (2) Schematic diagram of The pump components.

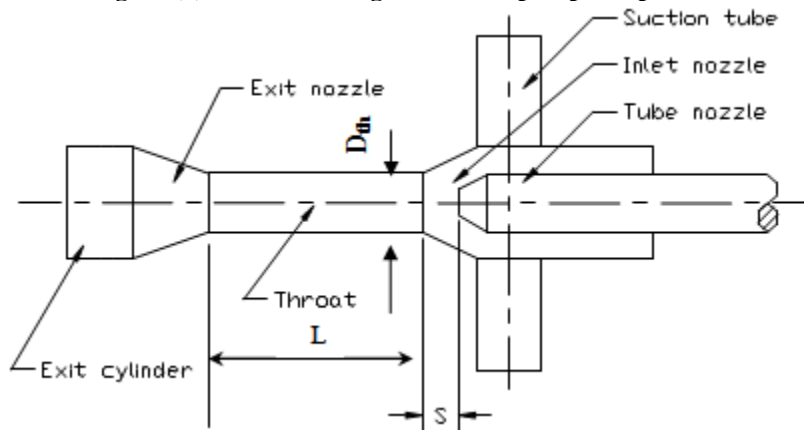


Figure (3) Schematic drawing of the convergent divergent tube of the jet- pump

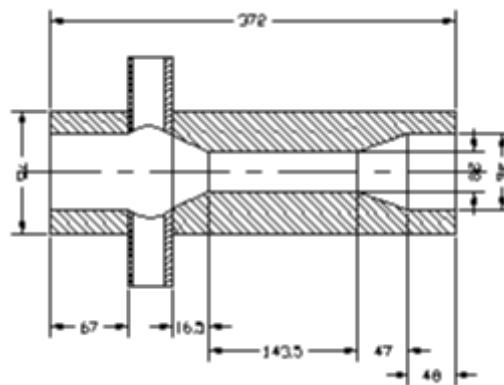


Figure (4) Schematic drawing of the lower flange of the pump assembly

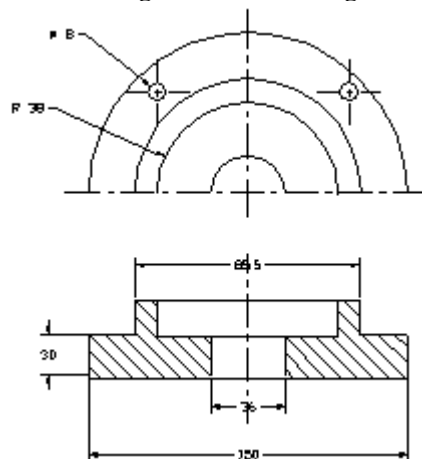
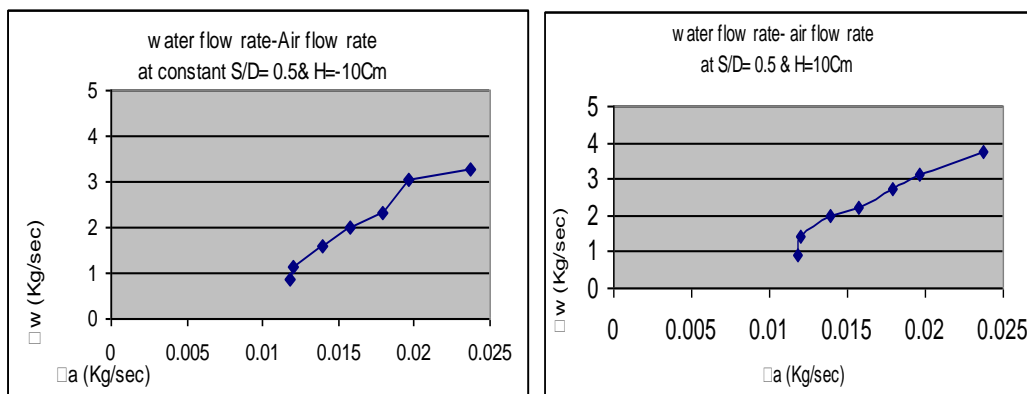
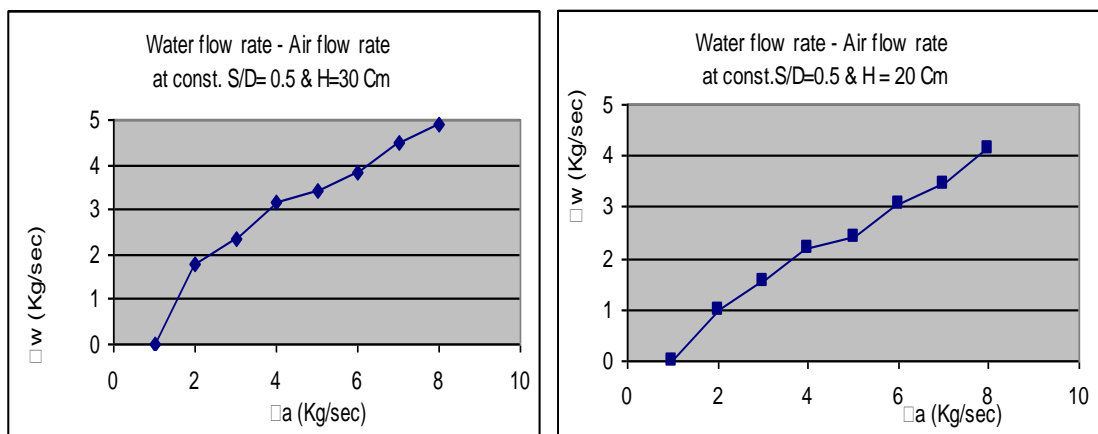


Fig. 8(a, b,c and d) Relation between discharge water mass flow rate and driving air mass flow rate at $S/D_{th} = 0.5$, $H_s = -10, 10, 20, 30$ Cm respectively for different values of suction heads



(a)

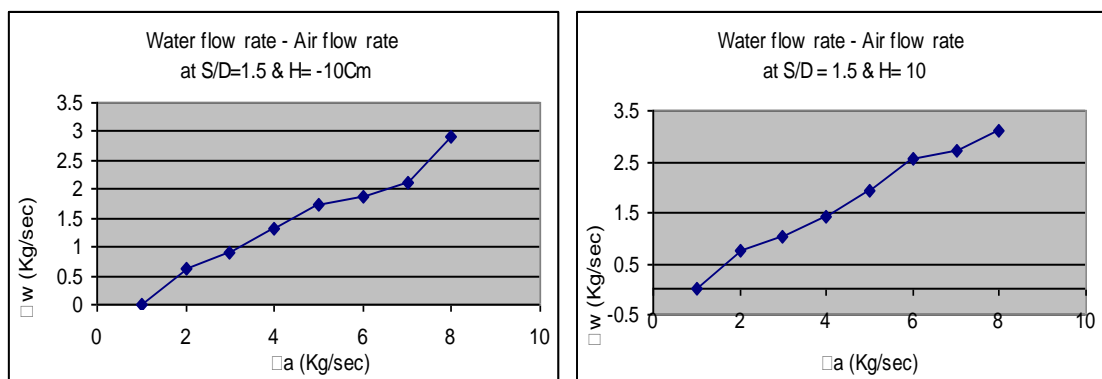
(b)



(c)

(d)

Fig. 9 (a, b,c and d) Relation between discharge water mass flow rate and driving air mass flow rate at $S/D_{th} = 1.5$, $H_s = -10, 10, 20, 30$ Cm respectively for different values of suction heads



(a)

(b)

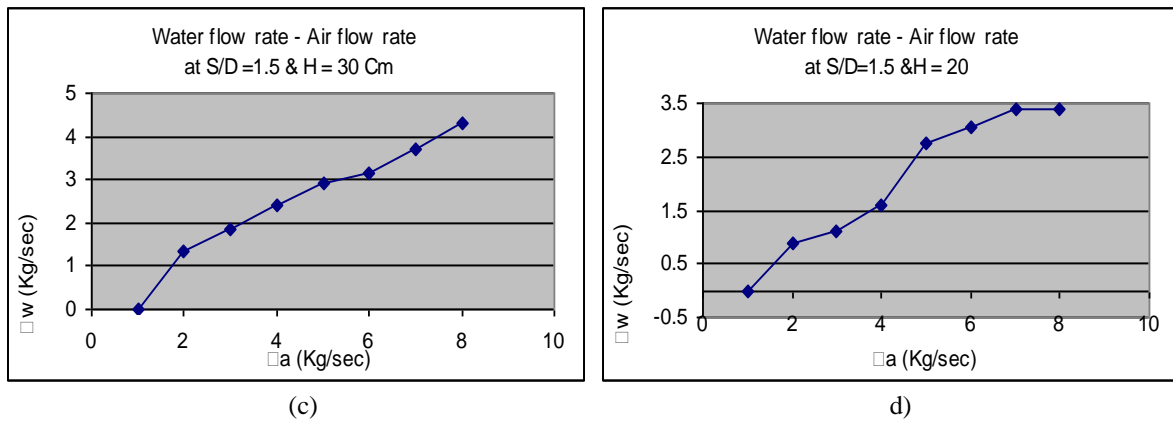
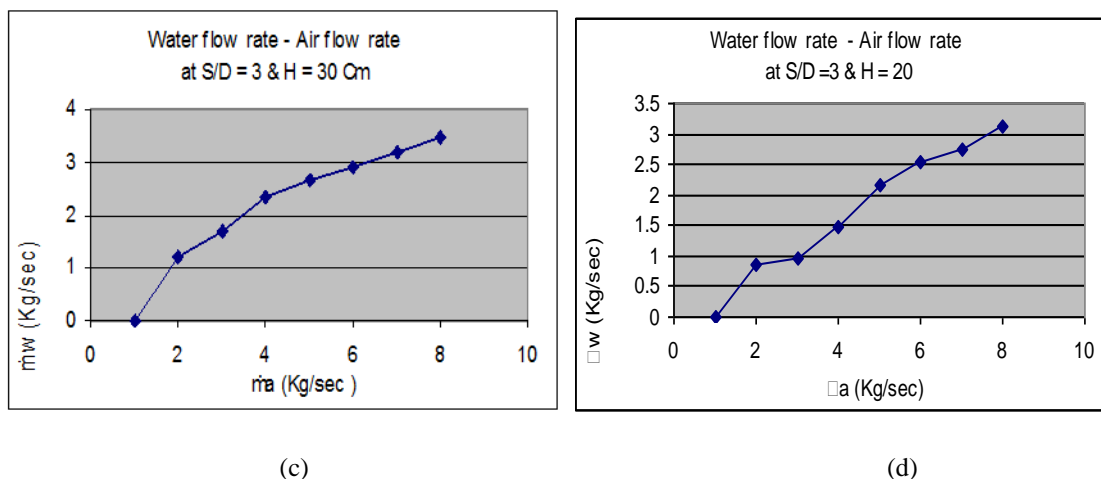
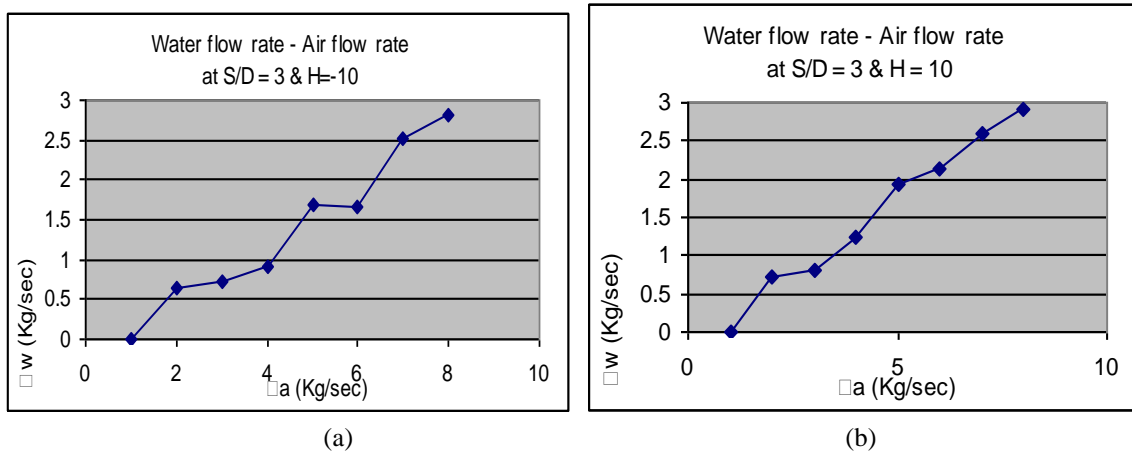


Fig.10 (a, b, c and d) Relation between discharge water mass flow rate and driving air mass flow rate at $S/D_{th} = 3.0$, $H_s = -10, 10, 20, 30$ Cm respectively for different values of suction heads



Nomenclature: -

| | |
|-------------------|--|
| A | Cross sectional area (m ²) |
| A _t | Total flow area (m ²) |
| A _n | Nozzle (jet) cross sectional area (m ²) |
| A _{MC} | Mixing chamber cross sectional area (m ²) |
| C _d | Calibration coefficient from the orifice calibration curve (-) |
| d _o | Orifice diameter (m ²) |
| D _{th} | Driving nozzle exit diameter (m ²) |
| D | Tube diameter (m ²) |
| D _{oi} | Orifice inside diameter (m) |
| D _{oo} | Orifice outside diameter (m) |
| D _{mix} | Mixing chamber diameter (m) |
| H | Static suction head (m) |
| H _s | Suction head is the net vertical distance between the water level in the feeding water tank and the center line of the suction tubes (m) |
| K | Constant (-) |
| Constant | |
| K _{en} | Friction loss coefficient, throat entrance (-) |
| L _{th} | Throat length (m) |
| (□ _a) | Air mass flow rate (m ³ /s) |
| (□ _w) | Water mass flow rate (m ³ /s) |
| M | Dimensionless flow ratio (m'_w / m'_a) (-) |
| n | Efficiency % |
| P _a | The driving air pressure "pressure of the jet of air coming from the nozzle (Pa) |
| P _{US} | Up-stream pressure (Pa) |
| P _{dS} | Down-stream pressure (Pa) |
| P _v | Vapor pressure (Pa) |
| R | Area ratio (A _n / A _{MC}) (-) |
| S | The distance between throat interface and driving nozzle interface (m) |
| t | Time (Sec) |
| T | Temperature (° C) |
| Z | High of water in the upper tank (Connected to the discharge line) (m) |
| α | Divergent or convergent angle (°) |